

Structural performance of timber frame joints – Full scale tests and numerical validation

S.A. Aeja^a, A.R. Dar^{*} and J.A. Bhat^b

Department of Civil Engineering, National Institute of Technology Srinagar, Hazratbal-190006 Jammu and Kashmir, India

(Received April 23, 2019, Revised December 13, 2019, Accepted December 20, 2019)

Abstract. The force resisting ability of a connection has direct implications on the overall response of a timber framed structure to various actions, thereby governing the integrity and safety of such constructions. The behavior of timber framed structures has been studied by many researchers by testing full-scale-connections in timber frames so as to establish consistent design provisions on the same. However, much emphasis in this approach has been unidirectional, that has focused on a particular connection configuration, with no research output stressing on the refinement of the existing connection details in order to optimize their performance. In this regard, addition of adhesive to dowelled timber connections is an economically effective technique that has a potential to improve their performance. Therefore, a comparative study to evaluate the performance of various full-scale timber frame Nailed connections (Bridled Tenon, Cross Halved, Dovetail Halved and Mortise Tenon) supplemented by adhesive with respect to Nailed-Only counterparts under tensile loading has been investigated in this paper. The load-deformation values measured have been used to calculate stiffness, load capacity and ductility in both the connection forms (with and without adhesion) which in turn have been compared to other configurations along with the observed failure modes. The observed load capacity of the tested models has also been compared to the design strengths predicted by National Design Specifications (NDS-2018) for timber construction. Additionally, the experimental behavior was validated by developing non-linear finite element models in ABAQUS. All the results showed incorporation of adhesive to be an efficient and an economical technique in significantly enhancing the performance of various timber nailed connections under tensile action. Thus, this research is novel in a sense that it not only explores the tensile behavior of different nailed joint configurations common in timber construction but also stresses on improvising the same in a logical manner hence making it distinctive in its approach.

Keywords: timber frame; joint configuration; tensile capacity; failure modes; bearing strength

1. Introduction

The significance of connection performance in the ability of a framed structure to resist forces arising due to diverse actions is indispensable. The concentration of stresses inherent to material discontinuity makes connections extremely damage susceptible thereby necessitating utmost concern to be divested in their design. Timber framed constructions involving various connection configurations have been used since times due to the sustainable, energy efficient, and light weight character of timber in contrast to contemporary building materials which are also by and large environmentally hazardous.

Tensile capacity is an essential property of timber-framed connections under pull-out / uplifting actions that has been investigated by many researchers to develop design guidelines and numerical models for strength prediction. However, attention in this area has been confined to pegged mortise-tenon connections wherein several parameters have been studied till date. The first

attempt to study the tensile behavior of pegged mortisetenon joints and frames experimentally as well as analytically was made by Brungraber (1985) in which the strength and stiffness was seen to enhance as the peg diameter increased. Kessel and Augustin (1995) also reported investigations on pegged mortise tenon joints involving evaluation of allowable loads for timber frame design under tension. In another study, peg failure was identified to be the most ductile mode when full scale mortise tenon joints were loaded in tension by Schmidt and Daniels (1999). Similar observations with peg diameter and shape having a significant influence on the failure mode were presented by Shanks *et al.* (2008).

The effect of joint fitness on the performance of pegged mortise tenon connections was explored by Bulleit *et al.* (1999) which revealed that peg suffered less damage in a tightly fit joint compared to a loose connection and that pegged joints can be modelled as pinned connections. Similarly, the effect of variation of end distance on the behavior of pegged mortise tenon joints under tension was reported by Burnett *et al.* (2003). In another study, the tensile capacity of varying angle pegged mortise tenon connections was evaluated by Walker *et al.* (2008) in which 45° connections exhibited the highest capacity followed by 90° and 67.5° connections respectively with connection stiffness reducing as the angle decreased. The work on angled mortise tenon connections was extended by Judd *et*

*Corresponding author, Professor

E-mail: abdulrashid@nitsri.net

^a Ph.D. Student

^b Professor

al. (2012) by developing a theoretical model for evaluating the tensile strength. Similarly, a finite element model in ANSYS based on the results of tensile testing of pegged mortise tenon connections was developed by Miller *et al* (2004).

Several researchers have also investigated the tensile behavior of mortise tenon joints assembled by fasteners of different materials instead of the conventional wooden pegs. Hasan *et al.* (2012) reported that GFRP dowelled mortise-tenon connections can be considered as a viable alternative to steel and wood dowelled connections because of the comparable performance of former in contrast to latter under tensile action. Similarly, a significant enhancement in the withdrawal capacity of round mortise tenon joints employing steel cross pins instead of wooden pins was observed by Eckelman *et al.* (2006) provided perpendicular to grain failure in the mortised member was prevented by reinforcement. In another study, splitting strength of the mortised member in the cross-grain direction considering the variation of edge distance and timber species by employing steel bolts instead of the wooden pegs was evaluated by Hindman *et al* (2016).

In contrast to pegged timber connections little research has been done on the nailed connections in the recent past despite extensive use of nails in timber construction. The load capacity prediction model for dowelled timber connections loaded normal to the fastener axis was developed by Johansen (1949) which considered embedded dowels as beam elements. Moller (1950) applied this model to symmetrical and unsymmetrical joints in single and double shear, which was later experimentally verified by Siimes (1954), Mack (1960) and Aune (1966). In another work, Larsen *et al.* (1969) reported substantial differences in the behavior of screw joints with respect to bolted joints in timber which was attributed to different values of embedment strength. The application of Johansen's model to nailed joint forms of different embedment strength was developed by Aune and Patton-Mallory (1986).

The bearing strength of steel-timber single dowel connections considering the influence of wood density and dowel friction was reported with proportional effects under tension by Dorn *et al* (2013). Similarly, the bearing strength of pegged connections in comparison to connections employing steel fasteners in various base materials was investigated by Church *et al.* (1997) and Wilkinson (1972) in two independent studies.

Though a lot of research has been done on pegged mortise joints and dowelled timber connections in the past but none of the work has studied various nailed joint configurations with an effort to refine the joint detailing by adhesive addition to compare the performance for optimization.

The primary purpose of the present research work is to conduct a comparative study for experimentally evaluating the tensile behavior of various nailed connection configurations supplemented by adhesive with respect to nailed-only counterparts, in order to ascertain the influence of adhesive addition on the connection performance. The experimental behavior has also been validated analytically by developing non-linear finite element models in

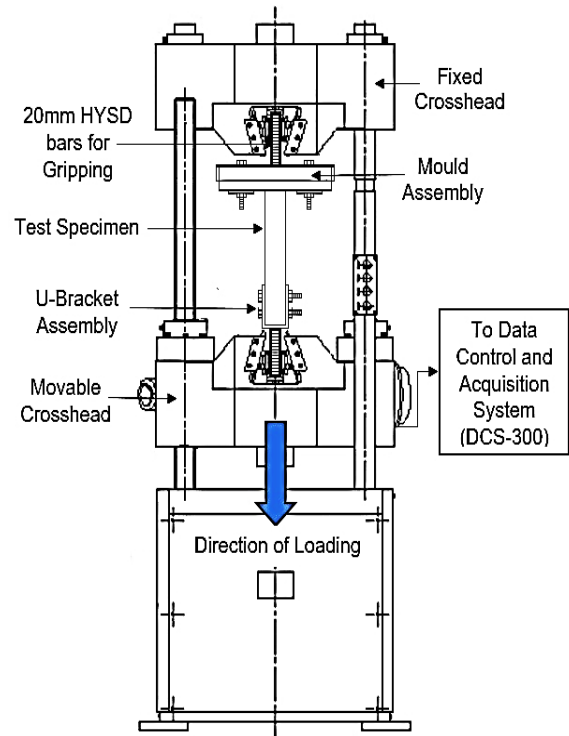


Fig. 1 Typical test specimen on a U.T.M.

Table 1 Properties of timber used

Property	Value
1. Specific Gravity	0.48
2. Moisture Content	12.56%
3. Modulus of Elasticity (MPa)	11218.41
4. Poisson's ratio	0.32
5. Tensile strength parallel to grain (MPa)	128.37
6. Tensile strength perpendicular to grain (MPa)	2.82

ABAQUS. Therefore, this study will not only facilitate in augmenting the meagre research in this area in recent past but will also aid in understanding the connection response so as to come across optimal performance under uplifting actions. The preliminary nature of this study suggests further work before implementation in design.

2. Experimental investigation

2.1 Test specimens

In this study, seasoned Fir (Budlu), common in traditional timber construction in Jammu and Kashmir, of sectional dimensions 70mm x 90mm (2.75" x 3.5") has been used for making full scale timber frame T-shaped connections. The timber properties evaluated as per IS-1708 (2005) specifications are given in the table 1 below:

Regular 62.5mm (2.5") iron nails and polyvinyl acetate which is a synthetic resin adhesive have been used to construct 16 specimens (4 each of Bridled-Tenon, Cross-Halved, Dovetail Halved and Mortise-Tenon configurations). Additionally, 12 specimens (3 each) of the

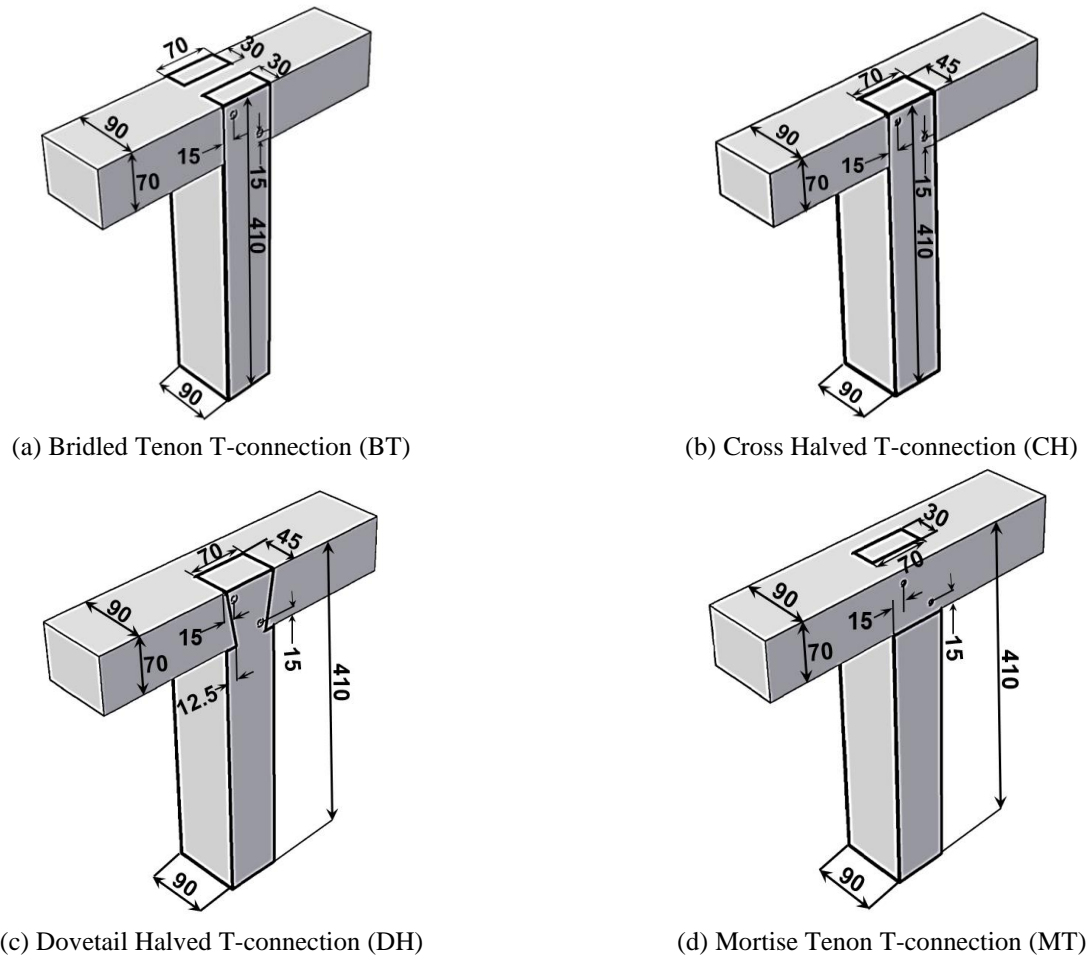


Fig. 2 Details of the connection types considered in this study (All dimensions in mm.)

aforementioned configurations have also been constructed keeping all the parameters same except the use of adhesive in order to ascertain its influence on the connection behavior.

2.2 Testing programme

The samples from the four connection types were tested on a Universal Testing Machine in displacement-controlled mode at a constant rate of 2mm/min for evaluating the tensile capacity under static conditions. The testing protocol included testing Nailed-Only connections followed by Adhesive cum Nailed connections from each configuration respectively. The testing of a typical T-connection on U.T.M. has been shown in Fig.1. In present research, the four T-connection configurations selected were based upon their common use in timber construction. The similar member dimensions of these connections enabled direct comparison, thereby facilitating the performance evaluation of the joint forms (with and without adhesion) individually, in addition to the various connection configurations considered. Thus, the present research is novel in a sense that it not only evaluates the structural behavior of Nailed Mortise-Tenon connection on which very little work has been done by the researchers in the past, but it also compares its performance to other configurations along

with the refinement in joint detailing by adhesive addition so as to establish quantitatively which connection profile behaves optimally. Such a study involving a quantitative comparative analysis of the structural performance of timber framed joints for optimization has not been undertaken till date, making this work innovative in its approach. The details of the connections considered in this research are shown in Fig.2.

For convenience and further reference, Nailed-Only connections in this work have been represented by two letters followed by a numeral code wherein letters denote the connection type and the numeral denotes the specimen number whereas Adhesive cum Nailed specimens have been differentiated from the Nailed-Only connections by a (*) symbol.

3. Results and outcomes

The test results have been presented in the form of Nailed-Only versus Adhesive cum Nailed connections for a particular joint configuration followed by comparison of various joint types in both the forms subsequently. Load-Deformation ($F-\delta$) plots have been used to evaluate the stiffness, load capacity and ductility of connections. Further, failure modes in various configurations have also been

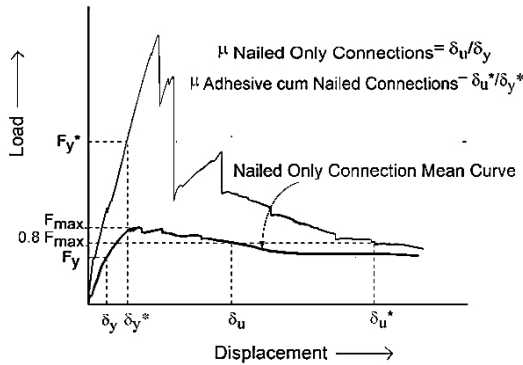


Fig. 3 Displacement-Ductility (μ) from a typical load-displacement curve

observed. The connection stiffness has been calculated based on the best fit to the initial portion of the F- δ plot from linear regression analysis. Similarly, the yield point has been defined based on the 5% diameter offset method specified in NDS (2018) wherein a line parallel to the initial stiffness at an offset of 5% connector diameter on the δ -axis intersecting the F- δ curve was considered.

The displacement-ductility (μ) in Nailed-Only connections has been defined as the ratio of the displacement corresponding to 80% peak load to the yielding displacement (Williams *et al.* 2008) whereas, in case of Adhesive cum Nailed connections, ductility was evaluated as the ratio of displacement at a point where the connection did not sustain a significant load to the displacement at yield (Judd *et al.* 2012) in which the point of insignificant load was taken as 80% peak load from the mean curve of the corresponding Nailed-Only counterpart (Fig.3). This definition gave the best interpretation as far as the comparative analysis of the joint forms with and without adhesion was concerned and was adopted since the load-displacement curves exhibited sharp load drops post peak point as a characteristic feature due to the detachment of the binding layer upon loading in Adhesive cum Nailed connections whereas, Nailed-Only connections showed a much gradual transition consequent to the lack of adhesion.

Additionally, evaluating displacement ductility corresponding to 80% peak load from the F- δ plots of Adhesive cum Nailed Connections would not represent the true behavior due to abrupt load drops resulting in very little ductility wherein the post drop portion load values being significant in comparison to Nailed-Only connections would be neglected.

3.1 Nailed Only Bridled Tenon (BT) vs. Adhesive cum Nailed Bridled Tenon (BT*) Connections

Both BT and BT* predominantly showed shear bearing failures compounded by complete tear out of the horizontal members in some specimen at large displacements under tensile loading. The F- δ plots revealed that BT* connections resisted very high loads in comparison to BT samples consequent to the largest bond area in adhesion. When loaded, detachment of the binding layer caused BT* to exhibit very sharp load drops but the enhancement in load capacity due to adhesive addition being highest when

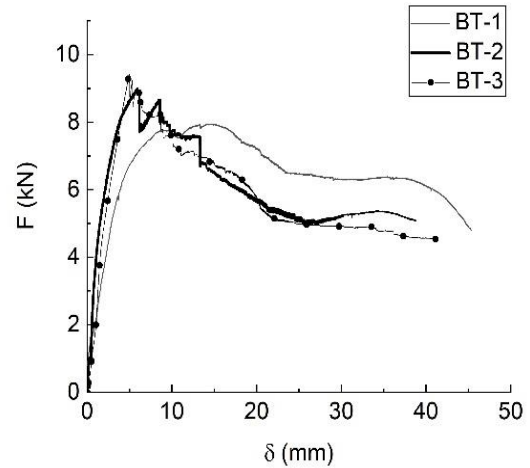


Fig. 4 F- δ plots of Nailed-Only Bridled Tenon joint

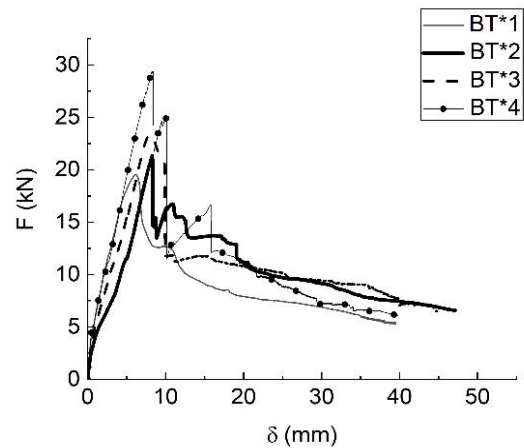


Fig. 5 F- δ plots of Adhesive cum Nailed Bridled Tenon joint

compared to other configurations overshadowed the former effect resulting in high ductility with respect to BT specimen. Additionally, BT* samples showed higher stiffness when referenced to BT. The F- δ plots of BT and BT* have been shown in Fig.4 and Fig.5 respectively along with the mean curves in Fig.6. The comparison of the mean curves showed that load capacity, stiffness and ductility enhanced by a factor of 2.49, 1.93 and 1.56 respectively by the use of adhesive in this connection configuration. The results evaluated have been tabulated below (Table 2) for both BT and BT* along with the mean values.

3.2 Nailed Only Cross Halved (CH) vs. Adhesive cum Nailed Cross Halved (CH*) Connections

Upon loading, CH and CH* connections primarily demonstrated bearing failure modes in which nails due to higher bearing strength crushed wood (softer material) along with samples CH*2 and CH*4 developing hairline cracks in both horizontal and vertical joint members. CH* connections showed significantly higher stiffness and load capacity with respect to CH connections wherein the enhancement in stiffness due to adhesive incorporation was the largest when compared to other configurations. The CH* connections also exhibited abrupt load drops (as seen

Table 2 Test results of nailed-only bridled tenon and adhesive cum nailed bridled tenon joints

Specimen	K (kN/mm)	F _y (kN)	δ _y (mm)	δ _u (mm)	F _{max} (kN)	F _{fail} (kN)	δ _{fail} (mm)	μ	Observed Failure Mode
BT-1	1.32	4.34	2.41	28.1	7.94	4.81	45.3	11.7	Shear Bearing + Cracking in the Horizontal Member
BT-2	1.61	4.86	1.44	13.4	8.98	5.08	38.8	9.30	Shear Bearing + Horizontal Member Tear Out
BT-3	2.04	5.43	2.28	10.1	9.42	4.53	41.3	4.43	Shear Bearing + Horizontal Member Tear Out
BT Mean	1.55	5.07	2.14	17.9	8.39	5.28	39.2	8.13	-----
BT*1	3.29	10.8	2.32	31.1	19.5	5.39	39.5	13.4	Shear Bearing + Hairline Cracks in Tongue of Vertical Member
BT*2	2.36	11.5	5.04	46.2	21.3	6.57	47.1	9.15	Shear Bearing + Tearing in the Horizontal Member
BT*3	2.89	11.0	3.25	44.6	23.2	6.48	44.7	13.7	Shear Bearing
BT*4	3.45	17.7	4.54	34.1	29.4	6.07	39.8	7.50	Shear Bearing + Complete Horizontal Member Tear Out
BT* Mean	2.99	10.4	3.07	38.9	20.9	6.69	38.8	12.7	-----

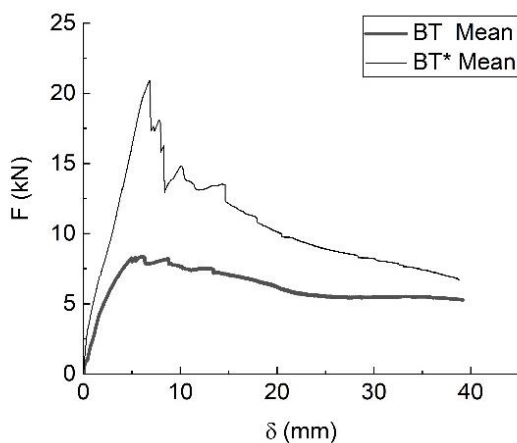


Fig. 6 Mean F-δ plots of Nailed-Only and Adhesive cum Nailed Bridled Tenon joints

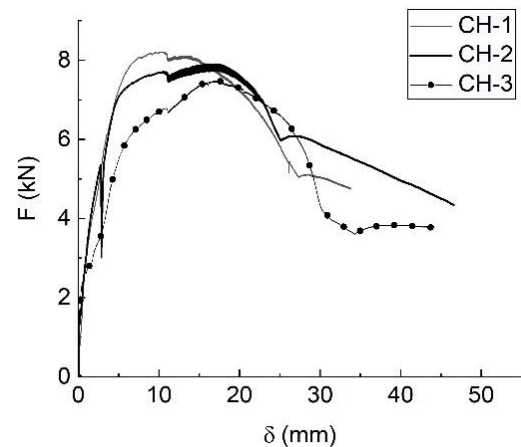


Fig. 7 F-δ plots of Nailed Only Cross Halved joint

in F-δ curves) in contrast to CH specimens wherein the load dropped very gradually thereby making ductility values of CH higher in comparison to CH*. Thus, the addition of adhesive was seen to impose adverse effects on the ductility in this connection configuration. The F-δ curves of CH and CH* are shown in Fig.7 and Fig.8 respectively along with the mean curves in Fig.9. On the mean scale, stiffness and load capacity improved by a factor of 2.71 and 1.73 respectively with the use of adhesive in this connection type, however ductility reduced by 28% when compared to CH. The results are presented in Table 3.

3.3 Nailed Only Dovetail Halved (DH) vs. Adhesive cum Nailed Dovetail Halved (DH*) Connections

DH and DH* specimens exhibited cross grain splitting in the horizontal T-joint members in conjunction with the

shear bearing failure mode consequent to nail induced compression. Despite the sudden load drop in the F-δ curves of DH*, considerable improvements in ductility were reported due to nearly plastic post-yield behavior when compared to DH connections. The cross-grain splitting in the horizontal joint members attributed to tenon-aper in this configuration was more pronounced in DH* connections than DH specimens and was seen to be linked to ductility thereby resulting in higher values in former when compared to latter. The F-δ plots are shown in Fig.10 and Fig. 11 with the mean curves in Fig.12. The use of adhesive did not contribute to a notable increment in the load capacity of DH* connections although stiffness showed a substantial increment with respect to DH specimens. The stiffness, ductility and load capacity of DH* exceeded DH by a factor of 2.40, 1.48 and 1.19 respectively when the average curves were considered. The results computed have been shown in Table 4.

Table 3 Test results of nailed-only cross halved and adhesive cum nailed cross halved joints

Specimen	K	(kN/mm)	F_y (kN)	δ_y (mm)	δ_u (mm)	$F_{max.}$ (kN)	F_{fail} (kN)	δ_{fail} (mm)	μ	Observed Failure Mode
CH-1	1.01		3.70	1.45	22.8	8.22	4.77	33.8	15.7	Shear Bearing
CH-2	1.06		3.91	1.43	24.2	7.91	4.34	46.6	17.0	Shear Bearing
CH-3	0.760		3.25	2.12	27.3	7.48	3.78	44.0	12.9	Shear Bearing + Cracking in the Tongue of Vertical Member
CH Mean	0.940		3.48	1.45	24.2	7.74	4.69	33.5	16.7	-----
CH*1	2.64		6.33	1.65	21.6	15.2	5.96	22.1	13.0	Shear Bearing
CH*2	4.14		3.90	1.19	16.1	17.5	3.91	23.0	13.5	Shear Bearing + Fine Cracking in the Horizontal and Vertical Member
CH*3	3.23		8.83	2.53	22.6	18.3	5.96	23.1	8.93	Shear Bearing
CH*4	2.58		7.39	1.42	25.2	17.6	5.77	26.5	17.7	Shear Bearing + Cracking of the Horizontal and Vertical Member
CH* Mean	2.55		7.15	1.79	21.3	13.4	6.16	21.4	11.9	-----

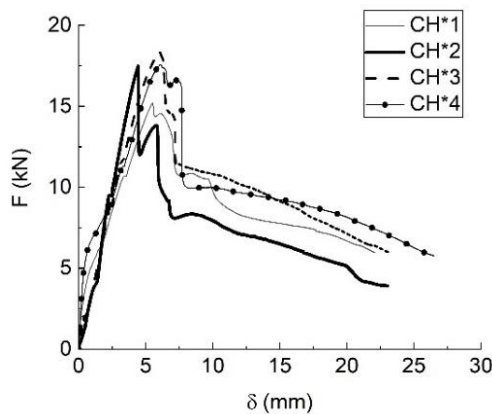
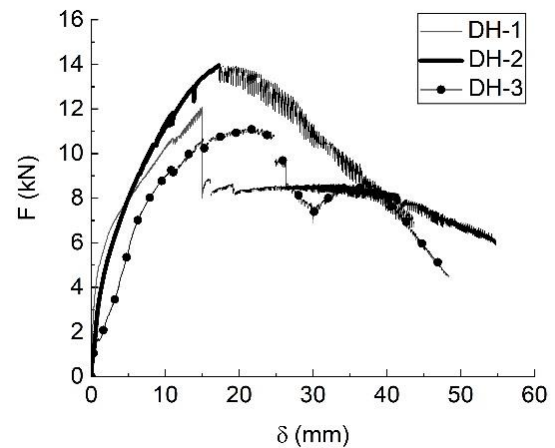
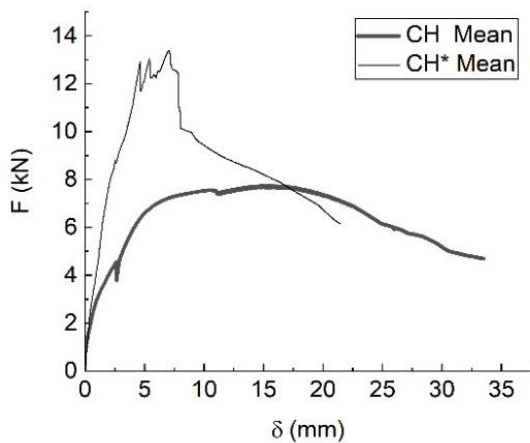
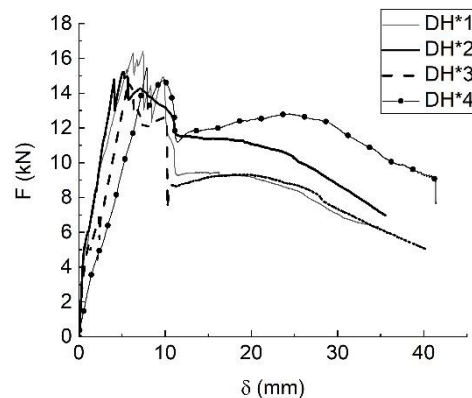
Fig. 8 F- δ plots of Adhesive cum Nailed Cross Halved jointFig. 10 F- δ plots of Nailed-Only Dovetail Halved jointFig. 9 Mean F- δ plots of Nailed-Only and Adhesive cum Nailed Cross Halved jointsFig. 11 F- δ plots Adhesive cum Nailed Dovetail Halved joint

Table 4 Test results of nailed-only dovetail halved and adhesive cum nailed dovetail halved joints

Specimen	K (kN/mm)	F _y (kN)	δ _y (mm)	δ _u (mm)	F _{max} (kN)	F _{fail} (kN)	δ _{fail} (mm)	μ	Observed Failure Mode
DH-1	1.04	5.22	1.26	15.0	12.1	6.01	54.8	11.9	Shear Bearing + High Cross Grain Splitting in Horizontal Member
DH-2	1.05	6.00	2.87	28.0	14.0	6.90	43.7	9.75	Shear Bearing + Cross Grain Splitting in Horizontal Member
DH-3	0.950	7.10	6.42	26.3	11.2	4.46	48.5	4.10	Shear Bearing + Cross Grain Splitting in Horizontal Member
DH Mean	0.990	5.14	2.67	26.2	12.1	6.96	44.0	9.83	-----
DH*1	2.41	7.78	1.68	11.1	16.4	6.30	34.8	6.64	Shear Bearing + Cross Grain Splitting in Horizontal Member + Cracking in Vertical Member
DH*2	3.44	7.14	1.52	27.2	15.2	6.98	35.5	17.9	Shear Bearing + Heavy Cross Grain Splitting in Horizontal Member
DH*3	2.29	6.39	2.04	10.2	14.6	5.00	40.4	5.00	Shear Bearing + Cross Grain Splitting in Horizontal Member + Cracking in the Tongue of Vertical Member
DH*4	1.85	7.65	4.12	38.8	15.5	7.75	41.4	9.40	Shear Bearing + Cross Grain Splitting in Horizontal Member
DH* Mean	2.38	6.53	1.84	26.9	14.3	8.62	30.5	14.6	-----

3.4 Nailed Only Mortise Tenon (MT) vs. Adhesive cum Nailed Mortise Tenon (MT*) Connections

MT and MT* connections mainly failed in bearing with the eventual tenon tear out in shear besides mortise splitting in a few specimen at large values of displacement. The F-δ plots are shown in Fig.13 and Fig.14. along with the mean curves in Fig.15. In contrast to other Adhesive cum Nailed configurations, incorporation of adhesive in this connection resulted in minimal enhancement in terms of stiffness, load capacity and ductility because of the confinement being imposed by the mortise sidewalls on the tenon, thereby, resulting in almost similar load capacity and ductility with a

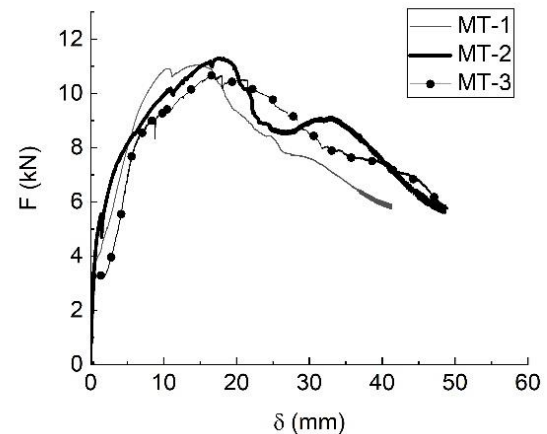


Fig. 13 F-δ plots of Nailed-Only Mortise Tenon joint

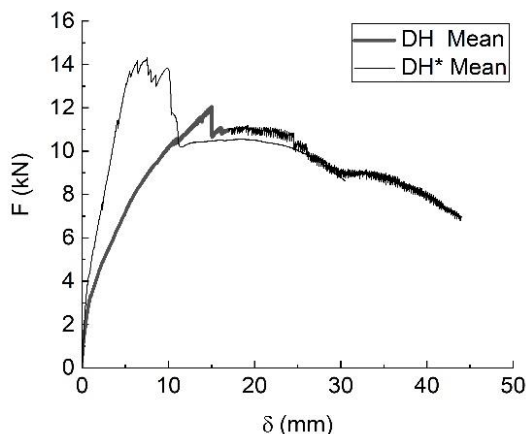


Fig. 12 Mean F-δ plots of Nailed-Only and Adhesive cum Nailed Dovetail Halved joints

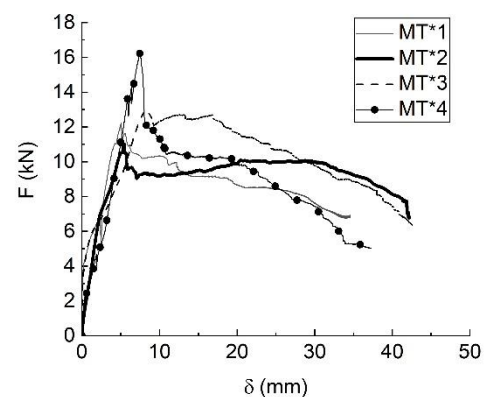


Fig. 14 F-δ plots of Adhesive cum Nailed Mortise Tenon joint

Table 5 Test results of nailed-only mortise tenon and adhesive cum nailed mortise tenon joints

Specimen	K(kN/mm)	F _y (kN)	δ _y (mm)	δ _u (mm)	F _{max} (kN)	F _{fail} (kN)	δ _{fail} (mm)	μ	Observed Failure Mode
MT-1	1.12	4.67	1.83	22.1	11.1	5.88	41.3	12.1	Shear Bearing
MT-2	1.24	5.18	1.13	23.0	11.3	5.63	48.7	20.4	Shear Bearing + Tenon Tear out in Shear
MT-3	1.18	4.82	3.64	29.8	10.7	5.74	49.0	8.21	Shear Bearing + Mortise Splitting
MT Mean	1.15	4.41	1.76	25.7	10.9	6.70	41.5	14.6	-----
MT*1	1.78	5.53	1.04	19.7	12.2	6.86	34.6	18.8	Shear Bearing + Mortise Splitting
MT*2	2.07	7.21	2.58	37.3	11.0	6.77	42.2	14.5	Shear Bearing + Tenon Tear out in Shear
MT*3	1.10	5.84	1.23	35.8	12.9	6.38	42.6	29.1	Shear Bearing + Tenon Tear out in Shear
MT*4	2.06	5.92	2.96	24.5	16.3	5.02	37.3	8.28	Shear Bearing + Tenon Tear out in Shear
MT* Mean	1.76	5.44	1.87	30.2	12.2	7.49	34.8	16.1	-----

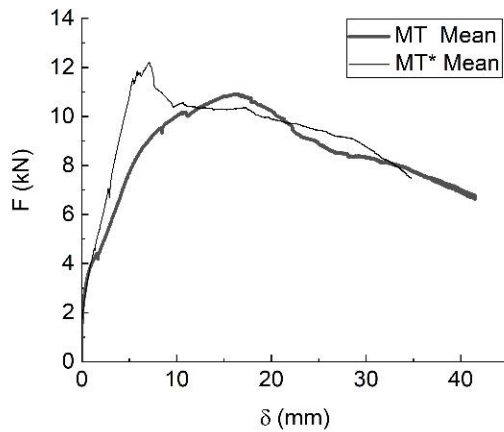


Fig. 15 Mean F-δ plots of Nailed-Only and Adhesive cum Nailed Mortise Tenon joints

marginal improvement in stiffness. The F-δ plots also revealed that MT* specimen did not exhibit very sharp load drops seen in other Adhesive cum Nailed configurations in this study. On comparing the mean curves stiffness, load capacity and ductility rose by a factor of 1.53, 1.12 and 1.11 respectively in MT* when referenced to MT. The results are presented in Table 5 below along with average values.

3.5 Comparison of T shaped nailed-only connections

The mean load-displacement curves used to evaluate the behavior of various nailed only connections considered in this study revealed that BT demonstrated the highest stiffness with limited load resistance and minimal ductility. The maximum ductility was shown by CH consequent to very gradual load drop despite exhibiting the lowest stiffness and load capacity in the group. DH noted with the largest load capacity showed lesser stiffness and ductility values. The performance of MT seen to be comparable to DH in terms of load capacity was reported with remarkable ductility and a relatively stiffer response when compared to the latter. Therefore, the optimum performance in the Nailed-Only category was shown by MT. The mean curves and the results are shown in Fig.16 and Table 7 respectively.

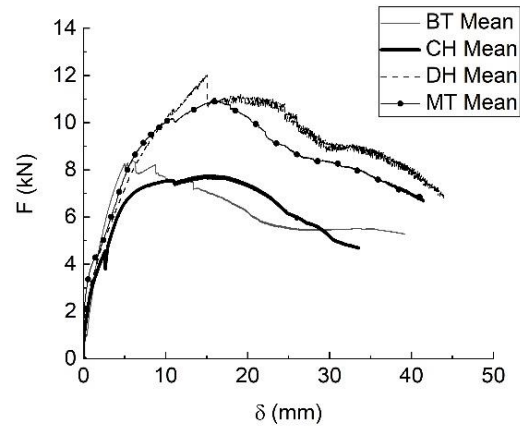


Fig. 16 Mean F-δ plots of Nailed-Only Joints

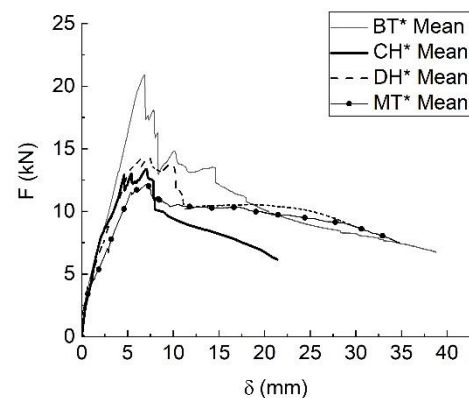


Fig. 17 Mean F-δ plots of Adhesive Cum Nailed Joints

3.6 Comparison of T shaped adhesive cum nailed connections

The incorporation of adhesive improvised the performance in terms of stiffness, load capacity and ductility in every configuration when referenced to its Nailed-Only counterpart except the ductility in CH* which was noted with adverse effects. It was observed from the mean F-δ curves that CH* showed the least ductile behavior with significant stiffness and meagre load resistance.

Table 6 Property enhancement factors with adhesive incorporation in various connections

Connection Type	K^*/K	F^*/F	μ^*/μ
Bridled Tenon	1.93	2.49	1.56
Cross Halved	2.71	1.73	0.720
Dovetail Halved	2.40	1.19	1.48
Mortise Tenon	1.53	1.12	1.11

Although, adhesive addition led to highest enhancement in the ductility of BT* when compared to other configurations, yet it demonstrated limited group ductility despite largest load capacity and stiffness. The lowest stiffness and load capacity seen in MT* was reported with maximum ductility. DH* exhibited comparable ductility to MT* with a much stiffer response and better load resistance. With considerable improvement in stiffness and ductility due to adhesion, the optimal performance in this category was shown by DH*. The mean curves along with the evaluated results are shown in Fig.17 and Table 7 respectively.



Fig. 18 Heavy Cross Grain Splitting in DH*2

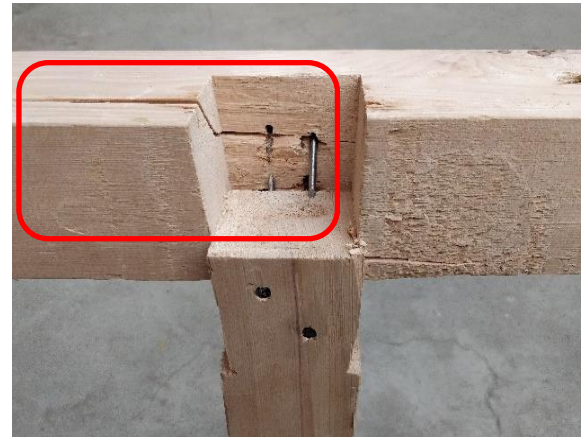


Fig. 21 Cross Grain Splitting in DH-1



Fig. 19 Horizontal Member Tear Out in BT*4



Fig. 22 Shear Bearing Failure in CH*2

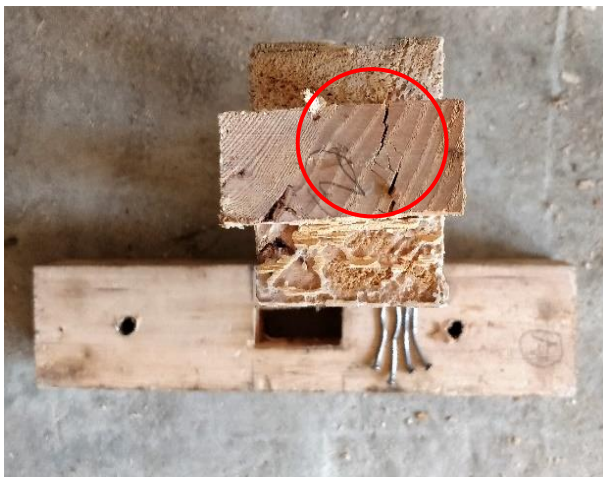


Fig. 20 Tenon Shear Tearing in MT*2



Fig. 23 Mortise Splitting in MT-3

Table 7 Mean test results of nailed-only and adhesive cum nailed joints

Specimen	K (kN/mm)	F _y (kN)	δ _y (mm)	δ _u (mm)	F _{max.} (kN)	F _{fail} (kN)	δ _{fail} (mm)	μ
BT Mean	1.55	5.07	2.14	17.9	8.39	5.28	39.2	8.13
CH Mean	0.940	3.48	1.45	24.2	7.74	4.69	33.5	16.7
DH Mean	0.990	5.14	2.67	26.2	12.1	6.96	44.0	9.83
MT Mean	1.15	4.41	1.76	25.7	10.9	6.70	41.5	14.6
BT* Mean	2.99	10.4	3.07	38.9	20.9	6.69	38.8	12.7
CH* Mean	2.55	7.15	1.79	21.3	13.4	6.16	21.4	11.9
DH* Mean	2.38	6.53	1.84	26.9	14.3	8.62	30.5	14.6
MT* Mean	1.76	5.44	1.87	30.2	12.2	7.49	34.8	16.1

Table 8 Predicted strength values for various connection types (F_{max.}) in kN

Connection Type	Yield Mode					
	I _m	I _s	II	III _m	III _s	IV
Bridled Tenon	23.3	23.3	N.A.	N.A.	8.93	<u>7.49</u>
Cross Halved	17.5	17.5	7.16	6.22	6.22	<u>3.73</u>
Dovetail Halved	17.5	17.5	7.16	6.22	6.22	<u>3.73</u>
Mortise Tenon	23.3	23.3	N.A.	N.A.	8.93	<u>7.49</u>

Note: The governing mode is shown underlined in bold for each connection type

4. Design strengths

The load capacity of single and double shear connections in the Nailed-Only category was predicted using limiting equations for the various yield modes specified in NDS (2018) from which the lowest computed strength was taken as the reference design value. The predicted values in LRFD (shown in Table 8), although, conservative, were fairly accurate in case of BT and MT connections but for CH and DH configurations overly conservative results were obtained when compared to mean experimental observations. The design strengths of Adhesive cum Nailed configurations could not be predicted because of lack of the relevant provisions in NDS (2018).

5. Numerical validation

The experimental behavior of connections was validated by modelling in ABAQUS v 6.13-1 using standard database platform which employed an implicit scheme of integration. Timber was modelled as an isotropic material using C3D8 solid elements by assigning the requisite mechanical properties obtained from prior testing. The isotropic representation of timber was justifiable because as per NDS (2018), small diameter dowels ($d < 1/4''$) in bearing exhibit strength invariance when load orientation with respect to grains is considered resulting in similar bearing capacity in any direction. Since all the connection configurations failed primarily in a bearing mode wherein timber crushed under nail induced compression ($d_{nails} = 3.38\text{mm}$), therefore, modelling timber as an isotropic material was a reasonable

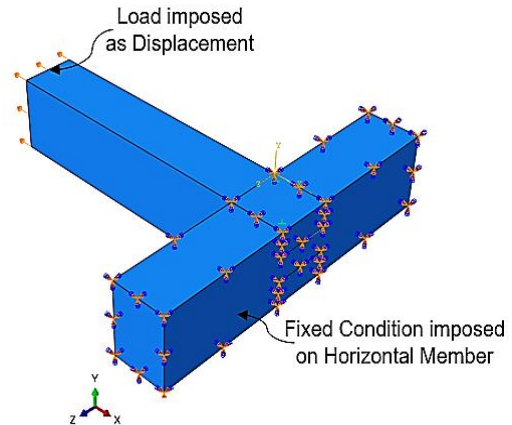


Fig. 24 Boundary conditions for bridled tenon joint

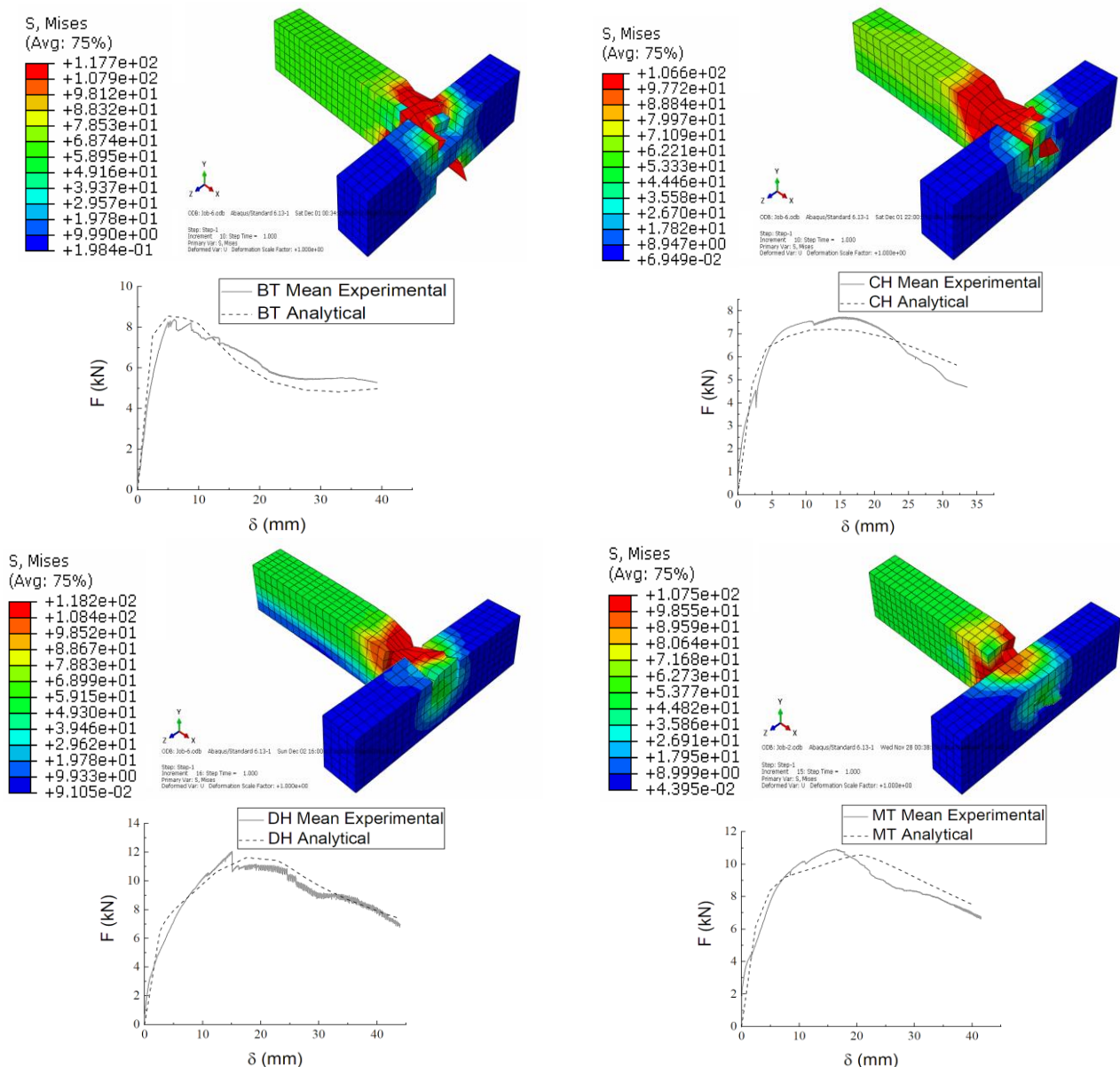
approximation that was further supported by the close match of analytical F-δ plots to the experimental curves.

The nails embedded in timber were modelled as 2-node beam elements under the assembled/complex category with all components of relative deformation in terms translation and rotation restrained. The adhesive layer in these connections was modelled by cohesive behavior option in the contact interaction property with default normal contact enforcement. Damage option was employed in conjunction with cohesive behavior interaction property to control the damage initiation and evolution.

In order to model the mechanical relationship between the surfaces in contact, standard surface to surface contact interaction was employed which included a reference to the interaction property created above. The binding between interfaces was represented by utilizing the concept of master and slave surface with small sliding formulation. In this, the surface nodes in the two regions formed a contact pair wherein every node on the slave surface was constrained to the same displacement value as the points on the master surface. Generally, ABAQUS selects the surface with high mesh refinement as slave surface in the analysis, however, in this modelling, both the master as well as the slave surface were assigned in a customized manner so that not only the computational cost reduced significantly, but, also the experimental outcomes were simulated in a better way.

The boundary conditions were imposed by fixing the horizontal member of the T-connection and applying load in the displacement-control mode (e.g. shown in Fig. 24 for BT) since the load-control option was faced with convergence problems. The mesh size was selected such that solution stability was ensured as high mesh refinement resulted in numerical instability. The connections were analyzed in the general static mode considering non-linear geometry effects for the default step time using full Newton solution technique. In Table 9, analytical F-δ curves extracted have been shown in comparison to the respective mean experimental plots along with the average Von-Mises stress contours for Nailed-Only connections followed by Adhesive cum Nailed connections. The results showed that the analytical curves were highly correlated to the observed experimental behavior, thereby, validating the same.

Table 9 Tensile stresses in various connection types along with the comparison of experimental and analytical plots



6. Conclusions and recommendations

This study helped in drawing the following conclusions:

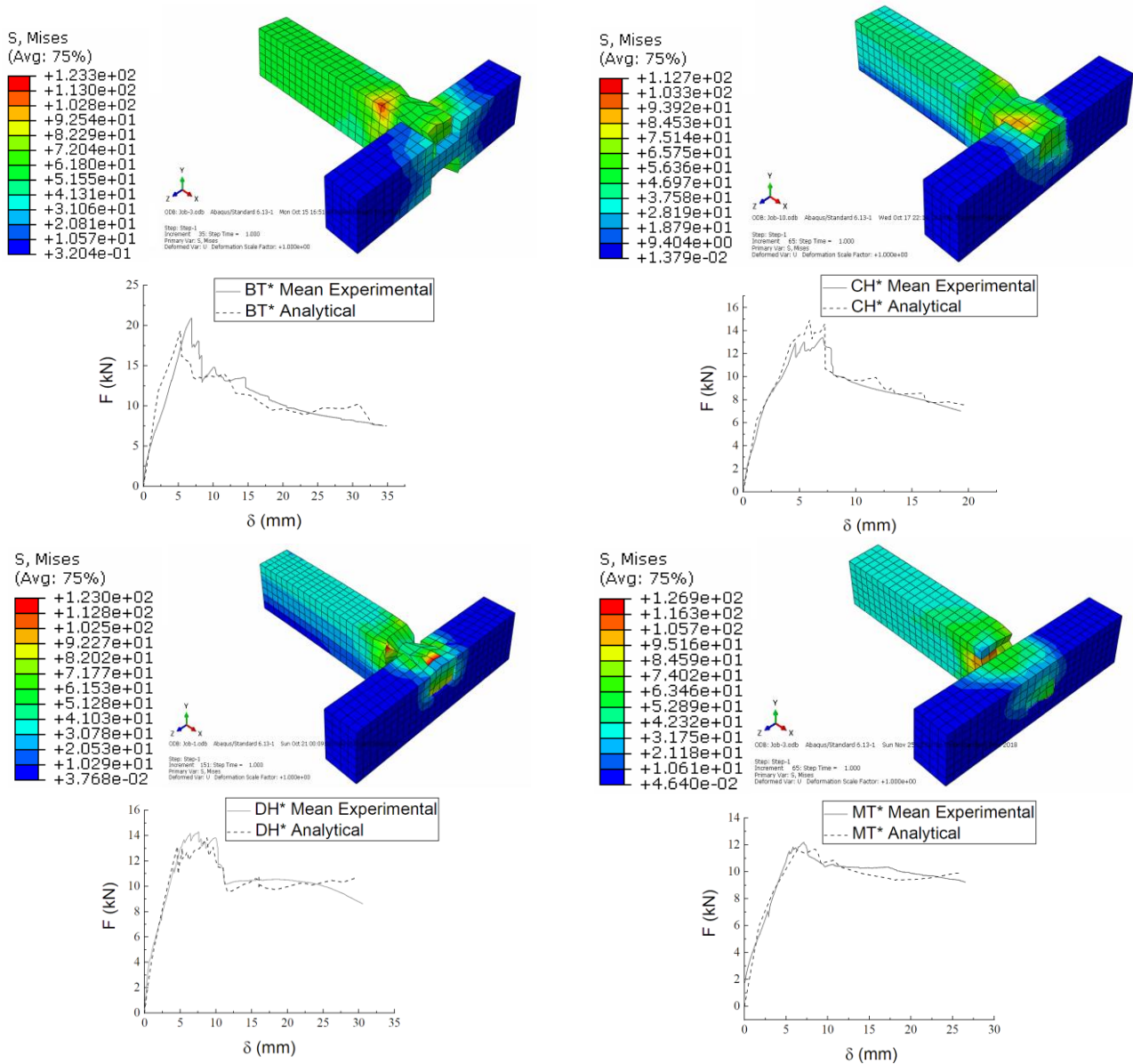
- Under tensile loading, all the Nailed-Only as well as Adhesive cum Nailed connections were seen to fail primarily in a shear bearing mode with eventual crushing consequent to the compression induced by pressing of nails against timber. This was obvious due to the higher bearing strength of nails with respect to timber and other failure modes observed in conjunction to shear-bearing at large displacements such as cross grain splitting, tenon shear tearing and complete member tear-out were regarded as secondary.

- Adhesive cum Nailed connections exhibited abrupt load drops post peak point as a characteristic feature in the load-displacement plots in comparison to Nailed-only connections wherein the load dropped gradually. This sharp load drop attributable to the detachment of binding

layer in Adhesive cum Nailed connections was seen to be the largest in Bridled Tenon and the least in Mortise Tenon configuration whereas the gradual transition in Nailed-Only connections was due to the lack of adhesion. The highest effect in Bridled Tenon was due to the largest bound area in adhesion whereas the lowest effect in Mortise Tenon was due to the confinement imposed by mortise side-walls on tenon.

- The incorporation of adhesive was observed to significantly improve the tensile performance of connections in terms of stiffness, peak load and ductility when compared to Nailed-Only counterparts except the ductility in CH* which dropped by 28%. Cross Halved configuration demonstrated the largest improvement in stiffness (2.71 times) with the highest enhancement in peak load (2.49 times) and ductility (1.56 times) seen in Bridled Tenon. Mortise Tenon exhibited the least improvement in stiffness (53%), load capacity (12%) and ductility (11%)

Table 9 (continued)



when compared to the Nailed-Only form which was obviously due to the confinement effect in this connection type.

- The highest stiffness (1.55 kN/mm), load capacity (12.1 kN) and ductility (16.7) in the Nailed-Only category was shown by Bridled Tenon, Dovetail Halved and Cross Halved connections respectively. Bridled Tenon displayed the least ductile behavior (8.13) with Cross Halved configuration demonstrating the lowest stiffness (0.940 kN/mm) and load capacity (7.74 kN) in the group. The optimum performance in this category was shown by Mortise-Tenon due to its comparable performance to Dovetail and Cross Halved configurations respectively in terms of load capacity and ductility along with a much stiffer response.

- The optimum performance in the Adhesive cum Nailed category was exhibited by Dovetail Halved configuration due to its ductile post yield behavior contrary

to Bridled-Tenon, despite highest group capacity (20.9 kN) and stiffness (2.99 kN/mm) of the latter. The most ductile behavior (16.1) of Mortise Tenon was reported with the lowest stiffness (1.76 kN/mm) and load capacity (12.2 kN) with Cross Halved configuration showing the lowest ductility (11.9) in this category.

- Cross grain splitting observed along with the shear bearing failure in Dovetail Halved connection was seen to be associated to ductility. This mode attributed to tenon-taper in this configuration was more pronounced in Adhesive cum Nailed connections compared to Nailed-Only counterparts thereby resulting in higher ductility in former with respect to latter.

- The predicted load capacity values from NDS (2018) were seen to be overly conservative in case of CH and DH connections although better estimates were obtained for BT and MT with all the configurations of the Nailed-Only category failing in yield mode IV. The design

values could not be predicted for Adhesive cum Nailed connections because of the lack of relevant provisions in this standard which may be incorporated in future.

- Due to small diameter dowels ($d < 1/4$ ") exhibiting similar bearing capacity irrespective of load orientation to grains, thus, modelling timber as an isotropic material in this study proved to be a reasonable approximation which was reflected by high correlation in the F - δ plots thereby validating the observed experimental behavior.

References

- ABAQUS User Manual v 6.13, Dassault Systèmes Simulia, Johnston, RI.
- ASTM F1575 (2017), Standard Test Method for Determining Bending Yield Moment of Nails, ASTM International, Pennsylvania, U.S.A. <https://doi.org/10.1520/f1575-01>
- Aune, P. (1966), *The Load Carrying Capacity of Nailed Joints. Calculations and Experiments*, The Norwegian Institute of Technology, Norway.
- Aune, P. and Patton-Mallory, M. (1986), *Lateral Load-Bearing Capacity of Nailed Joints Based on the Yield Theory: Theoretical Development*, Vol. 469, US Department of Agriculture, Forest Service, Forest Products Laboratory, U.S.A.
- Brungraber, R.L. (1985), "Traditional timber joining: A modern analysis", Ph.D. Dissertation, Stanford University, California, U.S.A.
- Bulleit, W.M., Sandberg, L.B., Drewek, M.W. and O'Bryant, T.L. (1999), "Behavior and modelling of wood-pegged timber frames", *J. Struct. Eng.*, **125**(1), 18707. [https://doi.org/10.1061/\(asce\)0733-9445\(1999\)125:1\(3\)](https://doi.org/10.1061/(asce)0733-9445(1999)125:1(3)).
- Burnett, D.T., Clouston, P., Damery, D.T. and Fisette, P. (2003), "Structural properties of pegged timber connections as affected by end distance", *Forest Products J.*, **53**(2), 50-57.
- Church, J.R. and Tew, B.W. (1997), "Characterisation of bearing strength factors in pegged timber connections", *J. Struct. Eng.*, **123**, 326-332. [https://doi.org/10.1061/\(asce\)0733-9445](https://doi.org/10.1061/(asce)0733-9445).
- Dorn, M., Borst, K.D. and Eberhardsteiner, J. (2013), "Experiments on dowel-type timber connections", *Eng. Struct.*, **47**, 67-80. <http://dx.doi.org/10.1016/j.engstruct.2012.09.010>.
- Eckelman, C.A., Haviarova, E. and Akcay, H. (2006), "Exploratory study of the withdrawal resistance of round mortise and tenon joints with steel pipe cross pins", *Forest Products J.*, **56**(11/12).
- Hassan, R., Ibrahim, A. and Ahmad, Z. (2012), "Experimental performance of mortise and tenon joint strengthened with glass fibre reinforced polymer under tensile load", *IEEE Symposium on Business, Engineering and Industrial Applications (ISBEIA)*, Bandung, Indonesia, September. <https://doi.org/10.1109/isbeia.2012.6423013>.
- Hindman, D and Milad, M. (2016), "Splitting strength of mortise members in timber frame joints", *J. Mater. Civil Eng.*, **28**(12). [https://doi.org/10.1061/\(ASCE\)MT.1943-5533.0001664](https://doi.org/10.1061/(ASCE)MT.1943-5533.0001664).
- IS:1708 (2005), Methods of Testing Clear Specimens of Timber, Indian Standards Institution, New Delhi, India.
- Johansen, K.W. (1949), "Theory of timber Connections", *International Association for Bridge and Structural Engineering*, **9**, 249-262.
- Judd, J.P., Fonseca, F.S., Walker, C.R., and Thorley, P.R. (2012), "Tensile strength of varied-angle mortise and tenon connections in timber frames", *J. Struct. Eng.*, **138**(5), 636-644. [https://doi.org/10.1061/\(ASCE\)ST.1943-541X.0000468](https://doi.org/10.1061/(ASCE)ST.1943-541X.0000468).
- Kessel, M.H. and Augustin, R. (1995), "Load behavior of connections with peg", *Timber Framing*, **38**, 6-9 and **39**, 8-10.

- Larsen, H. J. and Reestrup, V. (1969), "Tests on screws in wood", *Bygningssatiske Meddelelser*, **1**, 3-36.
- Mack, J.J. (1960), "The strength of nailed timber joints", *CSIRO Division of Forest Products*, TechNo. 9.
- Miller, J.F. and Schimdt, R.J. (2004), "Capacity of pegged mortise and tenon joinery", Report No. 50272; Timber Frame Business Council, Hamilton, MT, Timber Framers Guild, Becket, MA and University of Wyoming, Laramie, WY.
- Moller, T. (1950), "New method of estimating the bearing strength of nailed wood connections" Report No. 117; Gothenburg, Sweden.
- NDS (2018), National design specification for wood construction, American Wood Council, Virginia, U.S.
- Schmidt, R.J. and Daniels, C.E. (1999), "Design considerations for mortise and tenon connections", Report No. 9702896; USDA, NRI/CGP Washington DC and Timber Frame Business Council, New Hampshire, U.S.
- Shanks, J.D., Chang, W.S. and Komatsu, K. (2008), "Experimental study on mechanical performance of all-softwood pegged mortise and tenon connections", *Biosyst. Eng.*, **100**, 562-570. <https://doi.org/10.1016/j.biosystemseng.2008.03.012>.
- Siimes, F.E., Johanson, P.E. and Niskanen, E. (1954), "Investigations on the ultimate embedding stress and nail holding power of finish pine", *The State Institute for Technical Research*, Helsinki, Finland.
- Walker, C.R., Fonseca, F.S., Judd, J.P. and Thorley P.R. (2008), "Tensile capacity of timber-framed mortise and tenon connections", M.S. Dissertation, Brigham Young University, Utah, U.S.A.
- Wilkinson, T. L. (1972), "Analyses of nailed joints with dissimilar members", *J. Struct. Division, American Society of Civil Engineers*, **98**(ST9), 9189.
- Williams, M., Mohammad, M., Alexander, S. and Pierre, Q. (2008), "Determination of yield point and ductility of timber assemblies: In search for a harmonised approach", 10th WCTE, Japan, June.

CC

Notations

K	Stiffness
F_y	Yield load
δ_y	Yield displacement
δ_u	Displacement at insignificant load
F_{max}	Peak load
F_{fail}	Failure load
δ_{fail}	Failure displacement
μ	Displacement ductility
D	Diameter of dowel
F_{yb}	Yield strength of dowel in bending from ASTM F 1575 (2017) provisions
l_m	Dowel bearing length in main member
l_s	Dowel bearing length in side member
F_{em}	Dowel bearing strength of main member
F_{es}	Dowel bearing strength of side member
R_d	Reduction term
R_e	F_{em}/F_{es}
R_t	l_m/l_s

$$k_1 = \frac{\sqrt{R_e + 2R_e^2(1 + R_t + R_t^2) + R_t^2 R_e^3} - R_e(1 + R_t)}{1 + R_e}$$

$$k_2 = -1 + \sqrt{2(1 + R_e) + \frac{2F_{yb}(1 + 2R_e)D^2}{3F_{em}l_m^2}}$$

$$k_3 = -1 + \sqrt{\frac{2(1 + R_e)}{R_e} + \frac{2F_{yb}(1 + 2R_e)D^2}{3F_{em}l_s^2}}$$